Valve Characterization to Implement Feed-Forward Control of Hydraulically Actuated Joints

by
Abby Carey

SUBMITTED TO THE DEPARTMENT OF MECHANICAL ENGINEERING IN PARTIAL FULFILLMENT OF THE REQUIREMENTS FOR THE DEGREE OF

BACHELOR OF SCIENCE IN MECHANICAL ENGINEERING
AT THE
MASSACHUSETTS INSTITUTE OF TECHNOLOGY

June 2008

Signature of Author: _____
Department of Mechanical Engineering
May 9, 2008

Certified by: _____
Wai K. Cheng
Professor of Mechanical Engineering
Thesis Supervisor

Certified by: _____
Andreas Hofmann
Director of Machine Learning R&D, Vecna Technologies
Thesis Supervisor

Accepted by: _____
John H. Lienhard V.
Professor of Mechanical Engineering
Chairman, Undergraduate Thesis Committee

Valve Characterization to Implement Feed-Forward Control of Hydraulically Actuated Joints

by
Abby Carey

Submitted to the Department of Mechanical Engineering
on May 9, 2008 in partial fufillment of the
requirements for the Degree of Bachelor of Science in
Mechanical Engineering

Abstract

This thesis characterizes the flow behavior of a Hydraforce SP08-47CL valve given a specific pulse-width modulation (pwm) duty cycle. With a description of valve behavior, a feed-forward term can be implemented in the positional control loop of a hydraulically actuated robotic prototype. In order to isolate valve behavior, a test bed apparatus consisting of three separate hydraulic cylinders was constructed to decouple joint movement, and multiple tests were conducted, recording cylinder velocities given a constant pwm signal at a system pressure of 3.45MPa. After theoretically justifying the empirical results, a quadratic and bi-linear curve fit to the data provided a practical solution to an otherwise computationally expensive problem.

Thesis Supervisor: Wai K. Cheng
Title: Professor of Mechanical Engineering

Thesis Supervisor: Andreas Hofmann
Title: Director of Machine Learning R&D, Vecna Technologies

Acknowledgements

First and foremost, I would like to thank my thesis advisor, Wai Cheng, for encouraging me throughout the course of this off-campus thesis. Not only have you provided guidance during this one project, but you have supported me as an academic advisor during my entire undergraduate career in the Mechanical Engineering Department at MIT.

I would also like to thank Vecna Technolgies for their generous sponsorship throughout the duration of this thesis; never was there a moment when I was not given all of the supplies and advice needed to complete my work.

Specifically, I would like to thank Andreas Hofmann for proposing this particular project back in September; it was a fascinating cross between practical and theoretical work. Then, throughout the year, you provided a great deal of advice and direction that saved me many wasted hours.

Thank you to Josh Ornstein and Josh Young for all of your assistance on the electrical and programming ends. You both went above and beyond any reasonable amount of help I could have expected, and this thesis would not have happened otherwise.

Contents

List of Figures

List of Tables

1 Introduction

Vecna Technologies® is developing a Battlefield Extraction Assist Robot (BEAR™), capable of entering battlefields or natural disaster sites to retrieve human casualties. The demanding nature of traveling in hazardous regions with a fragile payload requires both a robust and accurate control scheme. The humanoid upper body consists of two arms with six degrees of freedom each; the lower body has been designed with four relatively identical tracked segments making up two humanoid legs with three degrees of freedom as seen in Figure 1. All joints are hydraulically actuated and controlled through valves manipulated by a pulse-width modulation (pwm) command signal. [1]

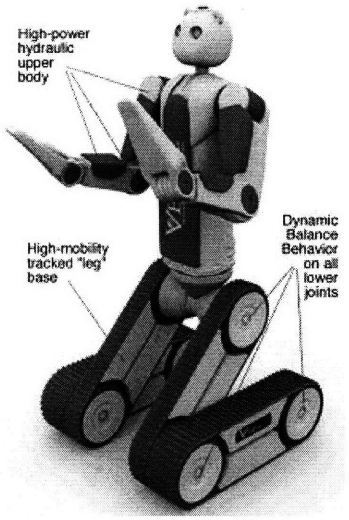

Figure 1: BEAR™, the Battlefield Extraction Assist Robot developed by Vecna Technologies®. The demanding nature of traveling in hazardous regions with a fragile payload requires both a robust and accurate control scheme. As each joint is hydraulically actuated and controlled with pulse-width modulation (pwm), one can accurately predict the flow rate into a hydraulic cylinder given a specific pwm signal, thereby improving upon the current positional control scheme.

Because of the strict requirements of accurate positional control, this thesis explores one potential method of improving upon the present positional control scheme. By accurately characterizing the behavior of the valves actuating each hydraulic joint, one can predict the

[1] Figure obtained from: *Product & services: The BEAR robot™*. (2007). Retrieved March 29, 2008, from http://vecnarobotics.com/robotics/product-services/bear-robot/bear_details.shtml.

resulting flow rate into the hydraulic cylinder, and subsequently, velocity and position of the joint, given a specific command signal. Inserting this empirical model of the valve into a feed-forward term in the control scheme will improve the path-following response of each joint by reducing error, overshoot, and delays.

2 Proposed Control Scheme

This thesis proposes to add a feed-forward velocity control term to the command signal into the valves in order to improve path-following capabilities of the BEAR^{TM} robot. While closing the loop via traditional feedback control on the valve command signal does solve such problems as correcting for deviations from a scripted path, several inherent problems in practical feedback control remain unchecked.

Theoretically, accurate positional control can be achieved by velocity control.[2] However, this is the case only in ideal systems; noise in fluid power systems traditionally manifest as pressure ripples due to, among others, cavitation, air in the system, broken seals, or damaged actuators.[3] In severe cases, noise has the potential for making a system become unstable.[4] Intuitively, noise in the system can greatly affect the output of any sensors being used in the control loop above and beyond the noise of the sensors alone. Employing this noise inside of the control loop will naturally affect the command signal given to the valves, producing steady state errors, overshoot, and oscillations that may have not been present in an ideal model.

Further, any type of feedback control necessarily has a time delay associated with motion. This delay may be inherent to the mechanical elements of the system-from extra

[2]R.B. Walters (1991). *Hydraulic and electro-hydraulic control systems.* Essex: Elsevier Science Publishers LTD, p. 35.

[3]J. Watton (2007). *Modelling, monitoring and diagnostic techniques for fluid power systems.* London: Springer-Verlag London Limited, p. 304.

[4]A. Akers, M. Gassman, & R. Smith. (2006). *Hydraulic power system analysis.* Boca Raton: Taylor & Francis Group, LLC, p. 335.

pressure required to overcome stiction in the cylinder to the finite time it takes a pressure wave to travel down a long pipe, or merely the required time for a large mass to respond to a command signal. Additionally, there will always be a delay on account of the computational time required to convert a sensor's analog output to a digital signal, combine it in a control law, and send a command signal. A true time delay—that is, a situation when "nothing [occurs] at the output" during the delay—reduces the phase margin of the system and leads to reduced stability.[5] Admittedly, none of the above examples may be large enough to dramatically affect stability, but applications wherein the controlled system is responsible for handling fragile payloads—such as humans—every reasonable effort must be made to improve the performance of the system.

One such effort would be to add a feed-forward velocity term in the control law, reducing the feedback term to positional correction rather than the primary command signal. Figures 2(a) and 2(b) contrast the difference between the two control schemes. Figure 2(a) describes a traditional feedback loop with proportional control; for this hydraulic system, the proportional control is on the position of each cylinder. For the reasons discussed above, a feedback element on the position must be included for accurate positional control.[6] Figure 2(b) shows a modified proportional control feedback loop with an additional feed-forward term included into the command signal. In the extreme that the plant output, y, perfectly follows the input signal, r, through the feed-forward term, the effect on the command signal due to the feedback loop is zero. One additional benefit is that any computational time delay or command signal variability due to noise is dramatically reduced.

A necessary element in utilizing the advantages of a feed-forward term in the control scheme is the ability to closely model the behavior of the plant being controlled. Without an accurate description of the plant behavior as a function of the command signal, the advantages of using the feed-forward term could be completely lost if the feedback loop must

[5]N. S. Nise. (2008). *Control systems engineering (5th ed.)*. Hoboken, NJ: Wiley, p. 660.
[6]Walters, p. 30.

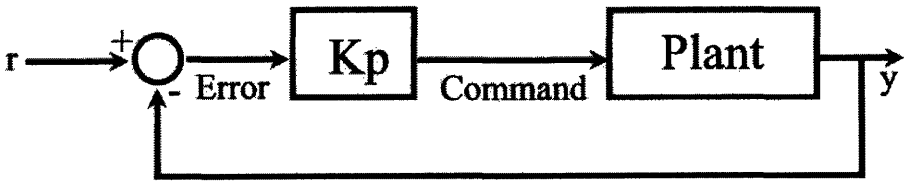

(a) A traditional proportional control block diagram.

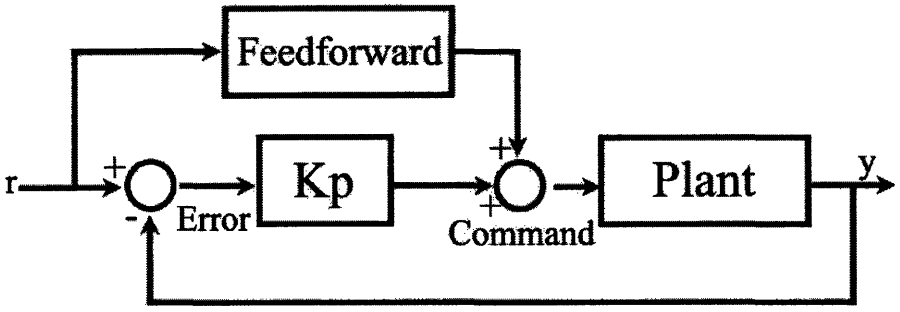

(b) Proportional control with an additional feed-forward term.

Figure 2: In the extreme that the plant output, y, perfectly follows the input signal, r, through the feed-forward term, the effect on the command signal due to the feedback loop is zero. One additional benefit is that any computational time delay or command signal variability due to noise is dramatically reduced. However, a necessary element in utilizing the advantages of a feed-forward term in the control scheme is the ability to closely model the behavior of the plant being controlled.

provide command signal corrections on the same order of magnitude as the feed-forward term. However, accurately developing a theoretical model of a system as complex as even simple hydraulic power systems is often an exercise in futility considering the practical limitations in closely modeling such variables as friction and stiction.[7]

Instead, by developing a set of empirically determined parameters describing the behavior of the plant—the valves controlling the hydraulic cylinders—with respect to such variables as system pressure and pwm signal, one may be able to employ the feed-forward term in the control scheme with as much success as could be achieved after developing a costly theoretical model of the plant.

[7]F. M. White. (2003). *Fluid mechanics (5th ed.)*. New York: McGraw-Hill, p. 343.

3 Test Bed Construction

In order to study the valves used on the BEAR^{TM} robot, a simpler test bed was constructed with three separate hydraulic cylinders representing three decoupled joints. The geometrical coupling of each extremity on the robot complicates any study of valve behavior alone; accurately representing the mechanical load on each joint as the cylinders move would require extensive–and expensive–modeling. Because this initial project looks only at the valve behavior, the additional expense was unnecessary. A test apparatus enabled one to decouple the motion of each joint as well as better control the mechanical loads exerted on each joint.

The test apparatus was designed to be general enough to carry out the current project experimentation as well as capably serve as a simple model of the robotic joints in the future. Because of the multiple degrees of freedom in each robot limb, the test bed consists of not one but three separate elements; Figure 3 is a solid model of one such element.

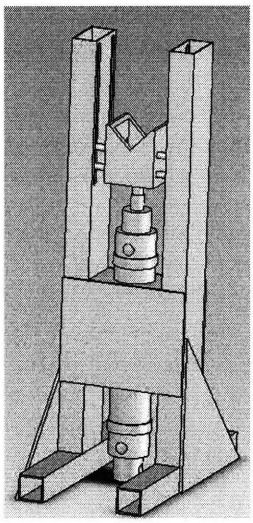

Figure 3: One section of the test bed setup. The test apparatus was designed to be general enough to carry out the current project experimentation as well as capably serve as a simple model of the robotic joints in the future. Because of the multiple degrees of freedom in each robot limb, the test bed consists of not one but three separate elements.

Each element holds a hydraulic cylinder upright and can be configured to support an addi-

tional mechanical load by means of a dumbbell weight set, seen in Figure 4. In addition to having used three different sized cylinders, the mechanical load for one of the test elements is suspended off-center via a lever to provide a varying mechanical load with cylinder position. By including an array of sensors similar to those on the actual robot on each cylinder, the test bed became a simple substitute for working with the robot given the requirements of this project.

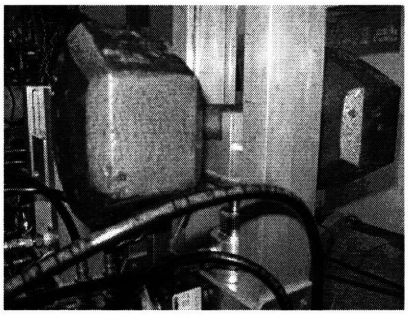

Figure 4: The test beds can be configured to support an additional mechanical load by means of a dumbbell weight set.

Each of the three Bimba hydraulic cylinders used in the test apparatus had a nominal maximum pressure of 3.45MPa (500 psi), identical to that used throughout testing. Based on the cross sectional area of the cylinde bore, then, the maximum load for the smallest cylinder, Cylinder A, was 2369N (533lbs), and 3614N (813lbs) for the two larger cylinders, Cylinders B and C. The piston travel is 0.102m, 0.102m, and 0.127m for Cylinders A, B, and C, respectively.

The Hydraforce SP08-47CL electro-proportional valves used on the test apparatus and throughout the BEAR torso are four way, three position valves with a closed center. They are energized by means of one of two solenoids, depending upon which direction flow is desired. With an operating pressure of 24.1MPa (3500psi), the valves predict a flow of 7.6lpm based on a 50% duty cycle.

The entire apparatus remains connected to the same pump and reservoir driving the actual BEAR^{TM} torso. Based on the maximum operating pressure of the cylinders, the pump

is controlled at a constant 3.45MPa throughout the experimental procedure. Hydraulic lines used between the pump and test apparatus are of 7.94mm (0.3125in) inner diameter, and brass elbows and fittings have an internal diameter of 6.35mm (0.25in). Figure 5(a) diagrams the placement of each of the cylinders with respect to each other and the pump.

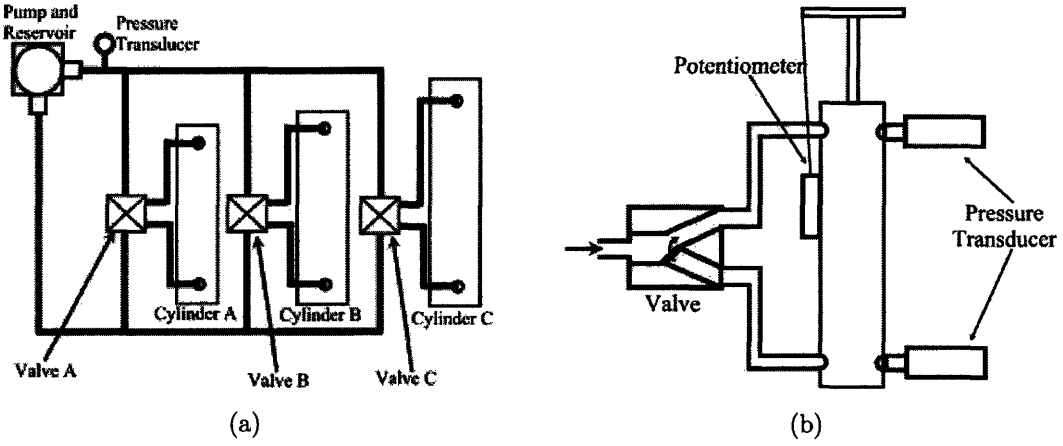

Figure 5: A schematic of the test bed setup. Figure (a) diagrams the placement of each of the three cylinders with respect to each other and the pump. Figure (b) shows the full sensor array included on each test cylinder. Potientometers are used to record the position of the cylinder piston, and pressure transducers were included for potential testing in later control schemes.

Figure 5(b) shows the full sensor array included on each test cylinder. Presently, BEAR^{TM} does not have the capability of recording the pressure on each side of the hydraulic actuators although there is a pressure transducer located behind the pump, depicted in Figure 5(a). As later prototypes of the BEAR^{TM} may include information such as the pressure differential across the cylinder in its control scheme, each hydraulic cylinder is customized to accommodate a pressure transducer at each port and will be utilized more in future testing. Potentiometers are used to record the position of the cylinder piston. The current software standardizes all joint positions by converting the travel of each piston into increments spanning -100 to 100; this method is implemented in the test bed apparatus since as much existing software as possible is utilized.

With these test cylinders, shown in Figure 6, one can develop an empirical model

of the valve behavior given different pump pressures, multiple joint movements, and varying mechanical loads. Initially, the project will examine valve behavior with pwm command signals for a constant pump pressure of 500 pounds per square inch (psi), or, 3.45 MPa. Additionally, while configured to operate multiple valves simultaneously, individual valves will first be tested. Overall, the generalized setup allows later control schemes to first be tested on this test apparatus without incurring undue risk to the actual BEAR^{TM} prototype.

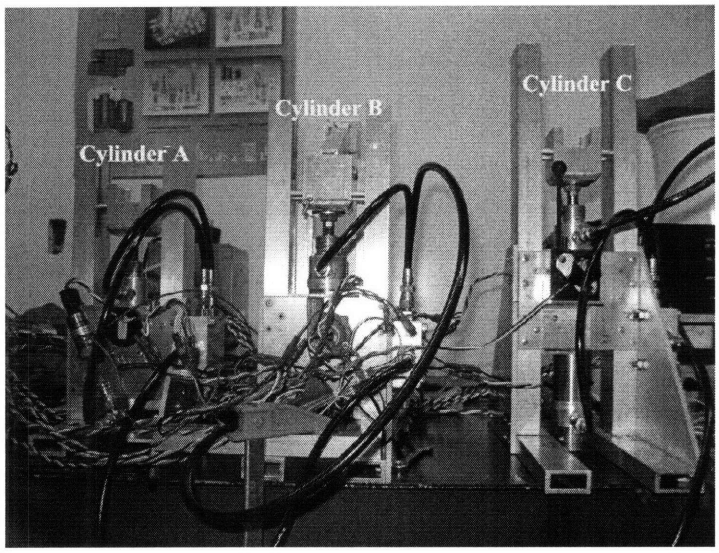

Figure 6: The complete test bed apparatus. With these test cylinders, one can develop an empirical model of the valve behavior given different pump pressures, multiple joint movements, and varying mechanical loads.

4 Experimental Methodology

4.1 Pump Control

The two elements being controlled in the test bed setup were the torso pump and the cylinder valves. The pump, although controlled independently from the valves and an analysis of which is not a part of this project, nevertheless had a direct impact on the quality of the data collected from the cylinders. During the beginning stages of data collection,

the pump used a simple proportional gain, set empirically, to maintain the desired system pressure. However, a too-large gain coupled with the wide variation in volumetric flow rates between one and three simultaneously actuated cylinders caused dramatic shifts in system pressure–upwards of 50 percent of the average value–as depicted below in Figure 7.

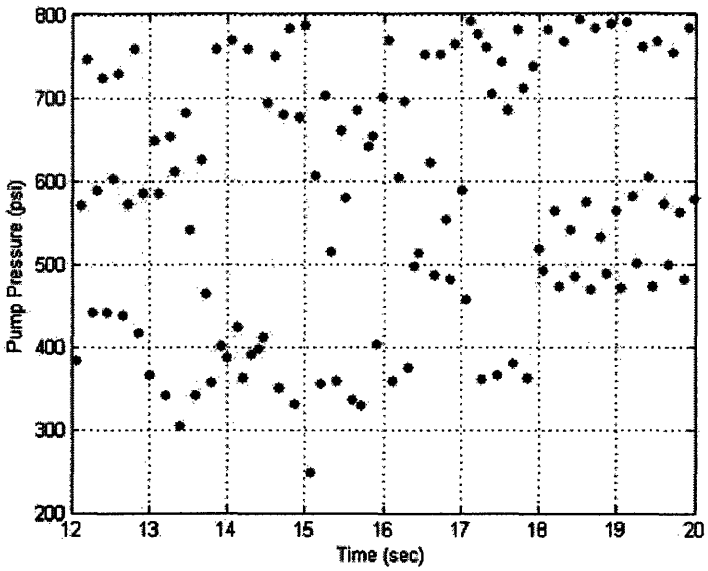

Figure 7: Initial pump noise with proportional control. During the beginning stages of data collection, the pump used a simple proportional gain, set empirically, to maintain the desired system pressure. However, a too–large gain coupled with the wide variation in volumetric flow rates between one and three simultaneously actuated cylinders caused dramatic shifts in system pressure–upwards of 50 percent of the average value.

Obtaining a smooth description of cylinder movement when the system was driven by such a wildly fluctuating pressure was difficult. Several unexpected nonlinearities were witnessed, at least partially caused by the system pressure. Figure 8 describes the resultant motion of cylinder A in response to opening the top valve at the nominal 500psi depicted above in Figure 7 and venting the bottom valve to the reservoir. Clearly, overcoming the stiction in the cylinder was beyond the capabilities of the system at that time, and the witnessed motion was that of irregular downward steps as opposed to a smoothly decreasing curve.

Only after the pump control scheme was improved was data collection able to be-

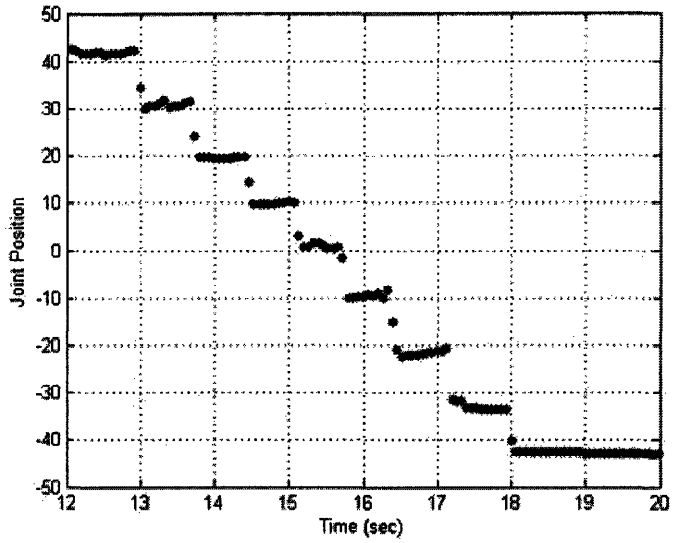

Figure 8: The resultant motion of cylinder A in response to opening the top valve at the nominal 500psi depicted above in Figure 7 and venting the bottom valve to the reservoir. Clearly, overcoming the stiction in the cylinder was beyond the capabilities of the system at that time, and the witnessed motion was that of irregular downward steps as opposed to a smoothly decreasing curve.

gin in earnest. As with all empirical tests, it is desirable to eliminate as many variables requiring explanation as possible, and while attributing the motion in Figure 8 solely due to the pressure of Figure 7 is not logical, eliminating the effect due to excessive pressure fluctuation is desirable. Figure 9 below shows a time course of the pump pressure, beginning at atmospheric pressure and increased to a nominal 500psi with an improved, variable gain controller. Fluctuation as a percentage of average value has decreased an order of magnitude from the original noise, and a qualitative improvement in cylinder movement was witnessed immediately.

4.2 Variable Payload Intention

After having eliminated one source of excessive noise in cylinder movement, initial tests to characterize the hydraulic valves began. The purpose of integrating dumbbells into the test bed configuration was to explore how different payloads affected cylinder performance.

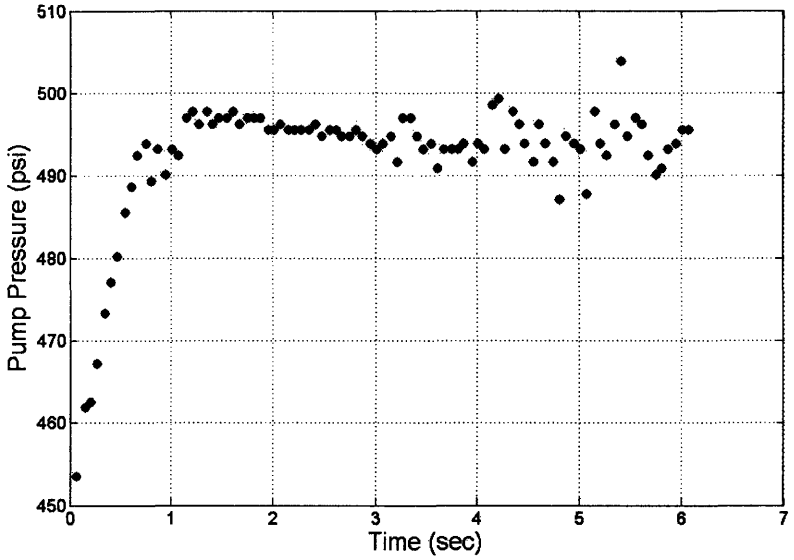

Figure 9: A time course of the pump pressure, beginning at atmospheric and increased to a nominal 500psi with an improved, variable gain controller. Fluctuation as a percentage of average value has decreased an order of magnitude from the original noise, and a qualitative improvement in cylinder movement was witnessed immediately.

Hypothetically, one could then develop a piecewise control scheme to, after determining the approximate weight of the load through pressure drops and flow rates, adjust according to the various weights. Too, cylinder B was built to include a moment arm such that the effective load on the cylinder varied with position. An unforeseen consequence in the project plan was how little the intended test weights–limited to 60lbs due to hardware considerations–would affect cylinder performance. Figure 10 plots the time course of cylinder A with simple proportional gain on an unmodified control scheme early during the test phase. Over the course of the ramp, the test run carrying no additional weight arrived at the final position only 0.061 sec earlier than the cylinder carrying 50 pounds–less than a ten percent difference over the duration of movement. Upon discovering this small effect, it was decided to neglect further exploration of weight variation during this initial test project. Consequently, all further tests described will be on cylinders carrying no additional weight unless specifically noted otherwise.

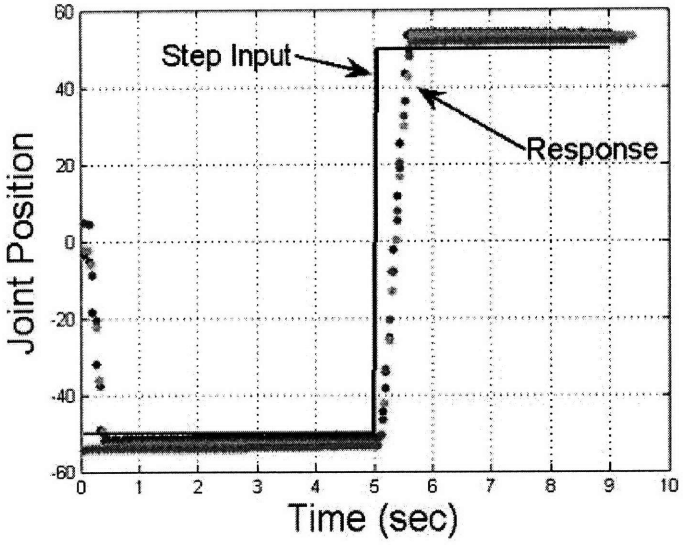

Figure 10: Cylinder A response to a step input carrying weights of zero, 10, 25, and 50 pounds on the initial, unmodified proportional control scheme. Note the different runs are nearly indistinguishable. Over the course of the ramp, the test run carrying no weight arrived at the final position only 0.061sec earlier than the cylinder carrying 50 pounds–less than a ten percent difference over the duration of movement. Upon discovering this small effect, it was decided to neglect further exploration of weight variation during the initial test project.

4.3 Motion Scripts

Presently used for testing and demonstration purposes, one feature of the current BEAR^{TM} software is the ability to upload text files describing a desired position at each joint along with a desired pump pressure; this was the primary method how movement requests were sent to each cylinder, or, joint. Testing and calibration modes enabled one to enter a desired position manually into the system, but the inability to control velocities reliably reduced these modes to simply ensuring the hardware function correctly.

Building a script entailed setting up a comma separated value (csv) file–converted from an Excel spreadsheet for this project–with one column each for expected time, joint position as described on the -100 to 100 scale used by the potentiometers, and pump pressure in closed loop control. Open loop control read the joint position columns as pulse-width modulation (pwm) duty cycles; rather than entering values from -100 to 100, pwm duty

cycles required entries from zero to 100. For the remainder of the described tests, the cylinders were operated in open loop control, with pwm command signals as the input.

4.4 Valve Characterization

The objective of these tests was to obtain an empirical description of how cylinder flow rate, and thus, cylinder velocity, varied with pwm signals so as to improve the path following capabilities of each joint. With that in mind, the first tests in open loop control were to obtain the smallest pwm duty cycle that overcame stiction in the cylinder–the dead zone. Sending a signal smaller than this minimum would not produce movement by definition. Therefore, each cylinder was isolated and given increasingly smaller duty cycles, beginning with a duty cycle of 50 and decreased in one-unit intervals. This test was repeated for all three cylinders, both ascending and descending.

Having obtained the smallest effective pwm signal, the cylinders were next set up to characterize the sensitive range of the duty cycles, or, the range of duty cycles through which the cylinder velocity increased. Each joint cylinder was individually driven with motion scripts dictating a constant pwm signal the entire length of travel allowed by hardware stops, both ascending and descending. Having determined previously that the minimum pwm duty cycle was approximately 40 for all three joints, the cylinders were run with scripts beginning at 40 and increasing in ten-unit intervals up to a duty cycle of 100, recording the pressure and position data for each test.

Figure 11 shows the results of this set of tests for cylinder C, plotting the average flow rate into the cylinder as a function of the command signal. Unexpectedly, the sensitive range of pwm signals looked qualitatively to exist between 40 and 60. As previous control schemes had been assuming the pwm signal was effective from zero to 100, these results provided encouraging evidence that the path following capabilities could be improved. Later theoretical discussion will explore the reason for the shape of the curve seen in the figure.

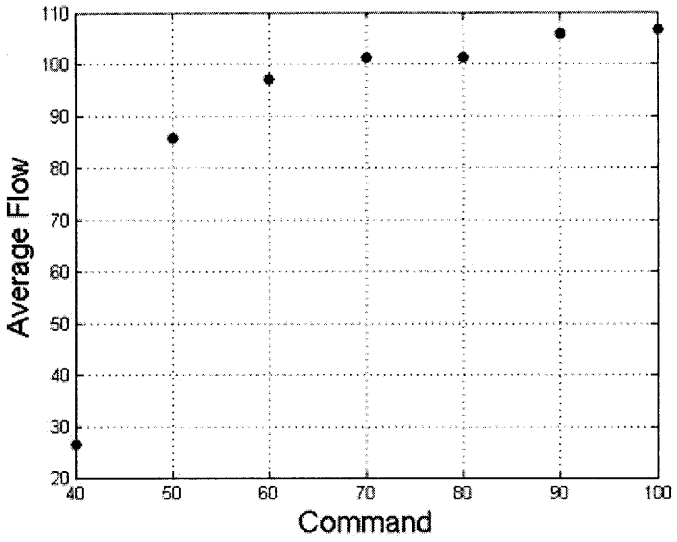

Figure 11: Average flow as a function of pwm command plotted for cylinder C. Unexpectedly, the sensitive range of pwm signals looked qualitatively to exist between 40 and 60. As previous control schemes had been assuming the pwm signal was effective from zero to 100, these results provided encouraging evidence that the path following capabilities could be improved.

However, having tested in pwm increments of ten, the test data did not provide enough resolution to accurately determine the relationship between flow rate and duty cycle. Therefore, a new set of motion scripts was built, again beginning at the smallest effective duty cycle and increasing this time by two through the qualitatively determined sensitive range, approximately 60. After again examining the resulting data, a third set of scripts ran each cylinder from its lowest value, increasing the pwm duty cycle by one through the most sensitive range, and then by three as the flow change tapered off. Figure 12 describes this final relation of cylinder velocity as a function of the pwm command signal for all three test cylinders. Note the effective range of the pwm duty cycles is only 20 percent that of the total potential range. Although this reduction decreases the resolution of potential desired velocities due to numerical round-off and the variability of friction, implementing this data into even a simple proportional control scheme will reduce the tendency of cylinders to lag behind the input until enough of a pwm signal is built up to overcome the initial dead zone.

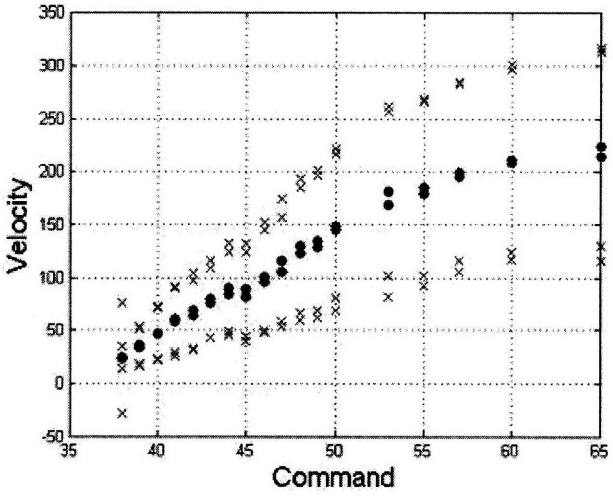

Figure 12: (a) Average cylinder velocity as a function of pwm command signal including standard deviations for cylinder A.

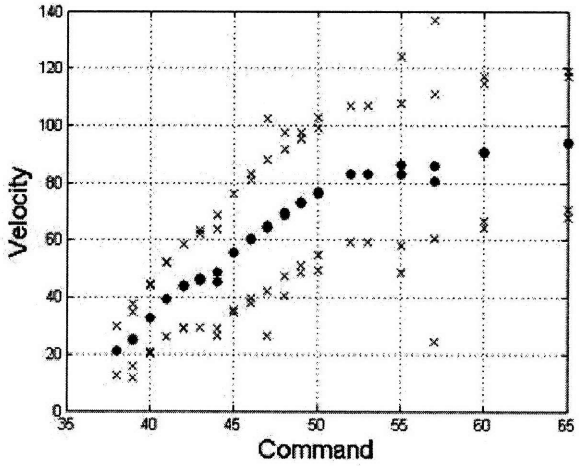

Figure 12: (b) Average cylinder velocity as a function of pwm command signal including standard deviations for cylinder B.

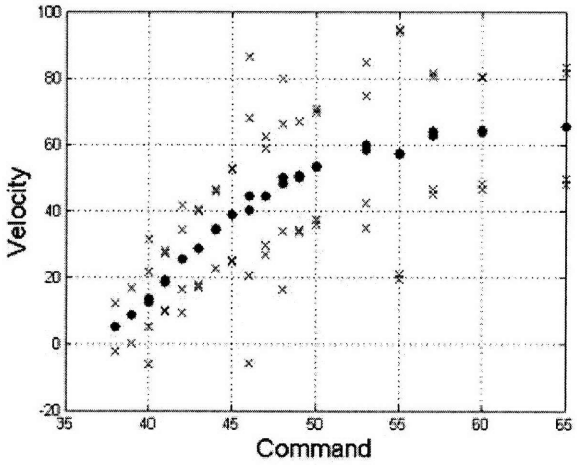

Figure 12: (c) Average cylinder velocity as a function of pwm command signal including standard deviations for cylinder C. After again examining the results from Figure 11, a third set of scripts ran each cylinder from its lowest value, increasing the pwm duty cycle by one through the most sensitive range, and then by three as the flow change tapered off. Note the effective range of the pwm duty cycles is only 20 percent that of the total potential range.

4.5 Data Manipulation Considerations

After collecting the data from motion tests, the raw sensor information required some collating and manipulation before analysis could begin. The pressure sensors did record the data directly in pounds per square inch (psi)–from which the drop across the valve could be found almost instantly–but joint velocity was not as immediate. As described previously, the travel length of each cylinder was broken into 200 steps spanning -100 to 100 and recorded as measured by the potentiometer. These positions were not converted back into SI units during analysis both for simplicity and to reduce numerical round-off error since the position and velocities would subsequently have to be converted back into this uniformly stepped scale when entered back into the scripting algorithm.

Further, the data collection rate of 50Hz described only the average time between each interval; in reality, the time steps differed up to 10% from each other. Characterizing this difference as significant, it was decided to maintain the uneven time steps in favor of a more accurate velocity calculation. Therefore, although the velocity vector as calculated

below in Equation 1 does not advance individually every 0.02sec, the average time increment remains consistent with the data collection rate of 50Hz. Also, there was necessarily a slight discrepancy between the time at which the clock was recorded and the time at with position or pressure was recorded. Considering the computational speed of the computers, this factor was dismissed as insignificant.

Calculating velocity from position was done by dividing a position difference, Δx, by a corresponding time step, Δt, and assigning the result to the time at which the later position was recorded, as seen in Equation 1.

$$\text{At } t_i,\ v_i = \frac{x_i - x_{i-1}}{t_i - t_{i-1}} \tag{1}$$

By definition, then, the length of the velocity vector was reduced to (n-1), and all motion scripts contained a minimum four second time period at the initial position to both allow the cylinders to travel to the beginning point and to ensure the initial velocities of cylinder motion during the resulting ramp were fully recorded.

5 Justification of Empirical Results

Having obtained an empirical model of cylinder velocity as a function of pwm command signal, an attempt can be made to justify the results seen in Figure 12. For simplicity, a single pump/pipeline/cylinder system is modeled as seen below in Figure 13.

Because the pump holds a constant pressure, P_1, it is modeled as a pressure source. The pipeline has area A_2, and immediately beyond the valve, the cylinder opens up to area A_c with unknown pressure P_c. Although a considerable approximation, the cylinder piston is modeled simply as a mass, m, with velocity v_c; the return side of the piston is given a constant pressure, assumed here to be atmospheric. An approximate Reynolds number calculation shows the fluid in the pipeline generally remains below the standard 2300 used

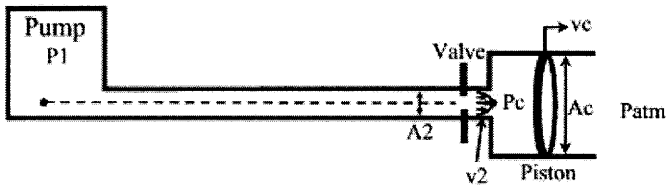

Figure 13: A theoretical model which one can use to quantitatively assess data collected from the cylinder test beds. The pump is modeled as a constant pressure source, the valve as having a variable loss coefficient, k, and the piston as a simple mass with a pressure differential. Combining Bernoulli's equation with a force summation will provide a relationship between the steady state velocity of the piston, v_c, and the loss coefficient, k, of the valve.

as transition from laminar to turbulence,[8] and the minor loss friction factor is then calculated at $\frac{64}{Re}$. Approximating the length of pipeline in the system as one meter with a diameter of 0.25", or, 6.35mm, it follows that the maximum loss coefficient due to minor losses will remain below ten. For computational simplicity, then, the variable loss coefficient, k, due to the valve alone is considered, and traditional major losses are neglected. However, a loss coefficient of 0.5 has been added in recognizance of the sharp exit from the pipe into the cylinder.[9] Conservation of mass combined with an incompressible fluid dictates the average velocity of the fluid inside the pipeline, v_2, is related to the velocity of the piston, v_c, by the ratio of areas.

With this simplified model, the steady Bernoulli equation will produce a relationship between pressure and piston velocity, described initially in Equation 2 and reduced in Equation 3.

$$\frac{P_1 - P_c}{\rho} + \frac{\cancel{v_1^2} - v_2^2}{2} + \cancel{g(z_1 - z_2)} = (\sum k_i + \frac{f\cancel{L}}{\cancel{D}})(\frac{v_{avg}^2}{2}) \tag{2}$$

$$\frac{P_1 - P_c}{\rho} - (\frac{A_c}{A_2})^2(\frac{v_c^2}{2}) = (k + 0.5)(\frac{A_c}{A_2})^2(\frac{v_c^2}{2}) \tag{3}$$

[8]White, p. 348, p. 353.
[9]White, p. 390.

Next considering the piston mass, Equation 4 relates the effect of the pressure difference and an added damping term, c, through force summation to the acceleration of the mass.

$$(P_2 - P_{atm})A_c - cv_c = m\frac{dv_c}{dt} \tag{4}$$

However, to find the steady state velocity, acceleration is here set to zero, and the simplified equation provides the additional relationship required between piston velocity and the pressure inside of the cylinder, seen in Equation 5.

$$P_2 = \frac{cv_c}{A_c} + P_{atm} \tag{5}$$

Combining Equations 3 and 5 into Equation 6, the steady state piston velocity can be reduced to the positive root of the quadratic equation with coefficients of the system parameters discussed earlier.

$$(\frac{A_c}{A_2})^2(\frac{k+2}{2})v_c^2 + (\frac{c}{A_c\rho})v_c + (\frac{P_{atm} - P_1}{\rho}) = 0 \tag{6}$$

Unfortunately, the variable loss coefficient, k, remains undefined, and a solution to Equation 6 would not provide the desired relationship between v_c and the pwm signal unless k could be found to depend directly on the pwm signal.

In order to develop this relationship, a model of the valve must next be built. The Hydraforce valves used during construction of the test fixture, pictured in Figure 14(a), enable flow through the various orifices by linearly manipulating a cover over one of the several holes spaced evenly around the valve circumference, a close-up of which is shown in Figure 14(b).[10]

Given no signal, the cover remains sealed over the entirety of the port, restricting

[10]Graphics obtained from: *Electro-proportional valves–directional control.* Retrieved February 12, 2008, from http://www.hydraforce.com/Proport/Prop-pdf/2-110-1.pdf

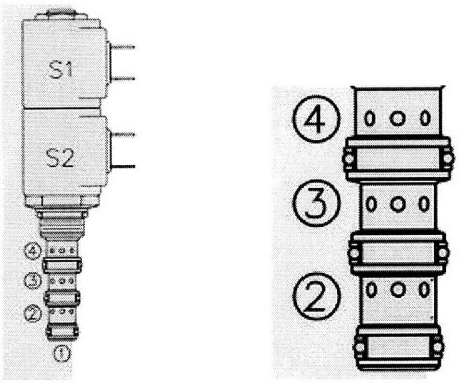

(a) (b)

Figure 14: The Hydraforce SP08-47C valves used during construction of the test bed fixtures. Flow is enabled through the various orifices by linearly manipulating a cover over one of the several holes spaced evenly around the valve circumference.

all flow to a nominal zero; upon receiving the maximum signal, the cover opens to allow maximum flow through one half of the area of the port. By definition, the average value of a signal, $\overline{y}$, is related to the duty cycle, D, through Equation 7. Here, the variable y represents the average value of the signal given a maximum at y_{max}, a minimum at y_{min}, and a duty cycle D.[11]

$$\overline{y} = Dy_{max} + (1 - D)y_{min} = Dy_{max} \tag{7}$$

Figure 15 relates the variable y to the geometry of the valve described above, and it becomes clear that the linear position of the valve cover is directly proportional to the pwm duty cycle.

Intuitively, one expects the loss coefficient to the valve to decrease as the port opening widens. Through chord geometry, Equation 8 describes the opened area of the half circle in Figure 15, A_{open}, as a function of the linear position of the cover, y, and the port radius, R.

[11]H. H. Asada. *Actuators and drive systems.* Unpublished manuscript, p. 8.

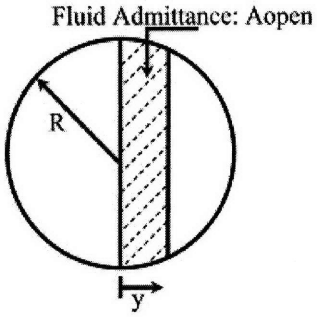

Figure 15: Given no signal, the valve cover remains sealed over the entirety of the port, restricting all flow to a nominal zero; upon receiving the maximum signal, the cover opens to allow flow through one half of the area of the port. The linear position of the valve cover is directly related to the duty cycle of the pwm signal.

Figure 16 subsequently plots Equation 8 as y increases from zero to R.

$$A_{open} = \frac{\pi R^2}{2} - R^2 cos^{-1}(\frac{y}{R}) + y\sqrt{R^2 - y^2} \tag{8}$$

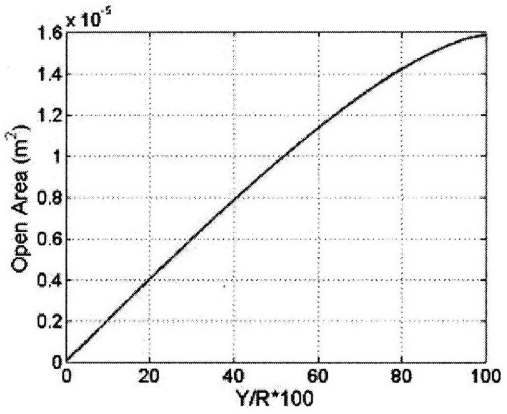

Figure 16: The relationship between the linear position of the valve cover, y, and the area of a valve opening through which fluid can flow, as described in Equation 8. The model here used a radius of 0.25in, or 0.00635m

Although intuition may suggest that k is inversely proportional to A_{open}, traditionally there exists no theoretical model between loss coefficients and various geometries due to the complexity of fluid dynamics; such relationships are found empirically.[12] Here, a relationship

[12]White, p. 343.

will be assumed. If after assuming a relationship the qualitative aspects of the theoretical model just developed differ dramatically from the empirical results obtained in Figure 12, one would have to iteratively return to the various assumptions made before a confident assertion could be made that the data collected provides a reasonable description of the variables in question: v_c and pwm command.

In a first order approximation, the loss coefficient is assumed to vary inversely with A_{open}, as in Equation 9; the constant C is simply a scaling factor.

$$k = \frac{C}{(A_{open})^n} \tag{9}$$

With the direct effect of y on k quantitatively assumed, Equation 6 can now be solved for the relationship between piston velocity and pwm command signal. The system variables are assumed as follows: fluid constants ρ = 890 kgm^{-3}; system geometry A_c = 0.00114m^2, A_2 = 3.17e-5 m^2, P_1 = 3447 kPa, P_{atm} = 101 kPa; c = 0.02 kg-sec^{-1}; and k = 10 at $y = R$. The resulting steady state velocity as a function of y is plotted in Figure 17 for two values of n, scaled such that the final velocities are identical.

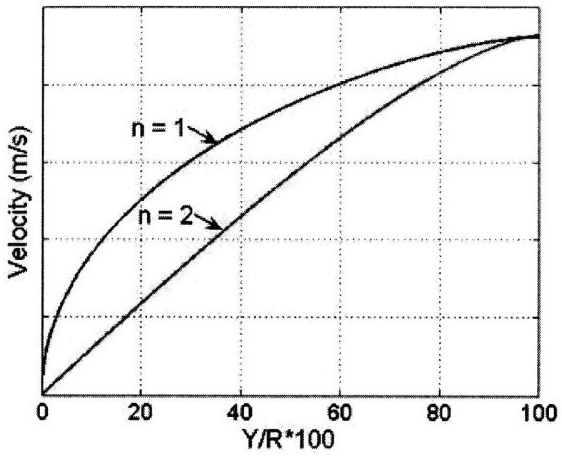

Figure 17: The steady state velocity of the piston as described by the theoretical model for differing relationships between the loss coefficient and the linear position of the valve cover. Particularly for the case $n = 1$, the shape of the plot does not match that of Figure 12, but important qualitative aspects–such as positive decreasing slope-are present.

Even though the theoretical model of Figure 13 simplifies the dynamics of the actual setup, Figure 17 demonstrates the empirical results obtained in Figure 12 are a reasonable description of the behavior of the piston velocity as a function of pwm command signal. Although the shape of the plot does not exactly match that of Figure 12, particularly for $n = 1$, the important qualitative characteristics are maintained: namely, that the slope is positive and decreasing with piston velocity. Unfortunately, this model does not capture the initial friction responsible for the dead zone nor does it describe the relatively narrow window wherein velocity can be effectively manipulated. A more complex, nonlinear behavior of friction could be developed in an effort to explain at least part of the discrepancies seen here, but given that the most efficient recourse would be to simply use the theoretical model to confirm the empirical results, as has been done here, further theoretical exploration will be left for another project.

6 Curve-fitting Empirical Results

Given that the behavior of Figure 12 has been theoretically justified as an accurate representation of the piston velocity and not the result of extraneous variables previously unconsidered, it remains to develop a convenient expression whose input is the desired cylinder velocity and the output the feed-forward command necessary to produce that velocity. Because the shape of the plots in Figure 12 look most like the plot in Figure 17 for $n = 2$, ideally, one would invert Equation 6 to solve for y as a function of v_c using $n = 2$ from Equation 9. However, the complex nature of A_{open} does not allow for a closed form solution of y. Instead, a quadratic polynomial and a bi-linear model will be fit to the data for each of the three cylinders, as shown in Figure 17.

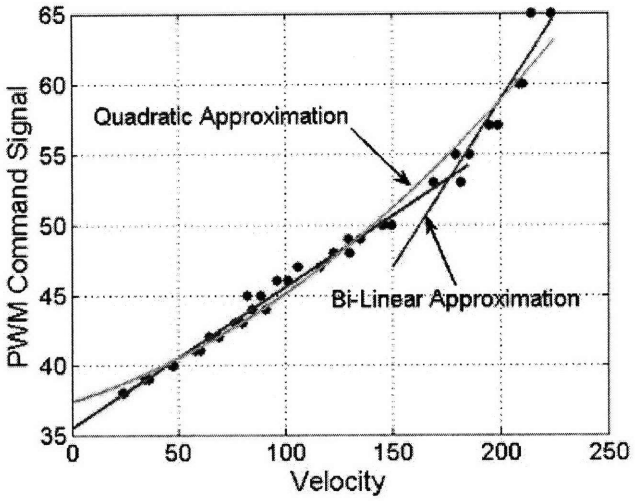

Figure 18: (a) Fitting curves to the pwm/velocity relationship for Cylinder A.

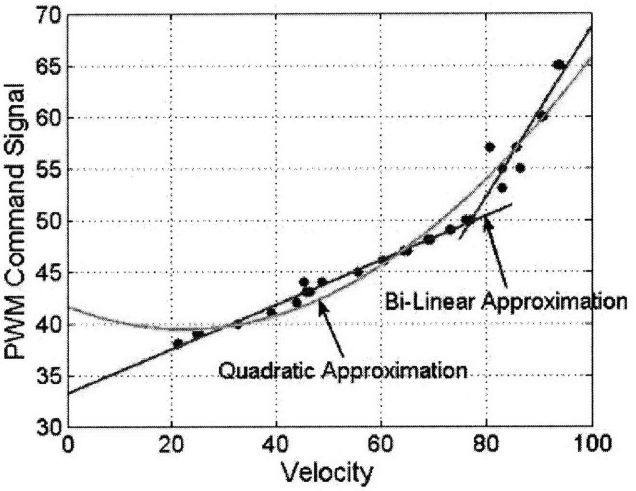

Figure 18: (b) Fitting curves to the pwm/velocity relationship for Cylinder B.

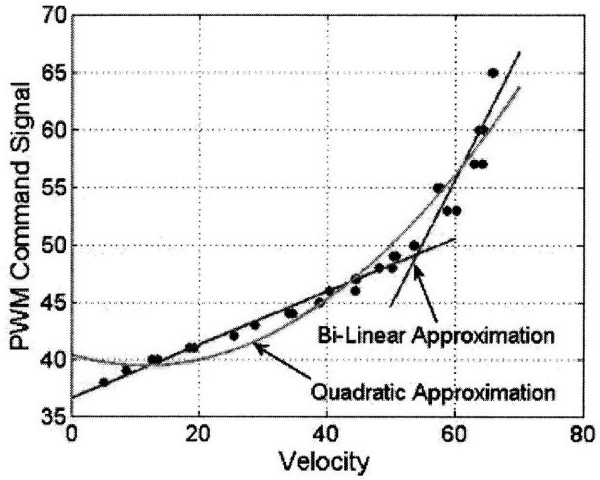

Figure 18: (c) Fitting curves to the pwm/velocity relationship for Cylinder C. Because the shape of the plots in Figure 12 look most like the plot in Figure 17 for $n = 2$, ideally, one would invert Equation 6 to solve for y as a function of v_c using $n = 2$ from Equation 9. However, the complex nature of A_{open} does not allow for a closed form solution of y. Instead, a quadratic polynomial and a bi-linear model will be fit to the data for each of the three cylinders

Table 1 describes the curve fits plotted against the data in Figure 18. As expected, the coefficients for all three cylinders are nominally similar, but note the downward turn of the quadratic equation and the increased slopes of the linear approximations for cylinders B and C. While Cylinder A had both a smaller bore and smaller travel distance, Cylinders B and C had identical bores but different travels. This would explain the relatively greater similarity between B and C when compared to A.

Further, dividing the different travel lengths into 200 identical segments necessarily implies an identical velocity in segments/second between the different cylinders results in an increasing velocity in m/sec with travel length. Due to current software considerations, as discussed earlier, it is more convenient to remain in units of segments/second as opposed to converting back to SI units in the interim. Eventually, the software of the BEAR™ robot will automatically convert the desired velocities into the necessary units, but with the current manual setup, Table 1 will be of more practical use.

	Bi-Linear Approximation	Quadratic Approximation
Cylinder A	$C = 35.45 + 0.101v$ $C = 11.27 + 0.238v$	$C = (2.95e-4)v^2 + 0.0480v + 37.35$
Cylinder B	$C = 33.21 + 0.214v$ $C = -13.71 + 0.823v$	$C = 0.00437v^20 - .198v + 41.65$
Cylinder C	$C = 36.59 + 0.233v$ $C = -10.74 + 1.107v$	$C = 0.00710v^2 - 0.164v + 40.37$

Table 1: The curve fits, pwm command C as a function of cylinder velocity v. Although the coefficients are nominally similar, note the downward turn of the quadratic equation and the increased slopes of the linear approximations for cylinders B and C. While Cylinder A had both a smaller bore and smaller travel distance, Cylinders B and C had identical bores but different travels. This would explain the relatively greater similarity between B and C when compared to A.

7 Future Considerations

Although this project was successful in accomplishing its goal of developing a relationship between cylinder velocity and pwm command signal, future experimentation would add depth and breadth to the above table. Due to hardware limitations, variable payload experiments were not carried out during the course of this project as discussed earlier. Modifying the test bed setup may enable an expansion of the feed-forward command signal tables to include mechanical load considerations. Particularly for this robotic application, the loads carried by the cylinders will vary anywhere from zero to an additional 500 pounds (2224N); the geometrical coupling also dictates that the effective load on each cylinder changes constantly with position. Intuition suggests that the response of a cylinder will vary with extreme load changes given a constant input signal. Therefore, it would be valuable to be able to estimate the load from sensor data and select the appropriate pwm command accordingly with some kind of force or impedance control.

Another extension of this project would be to explore the behavior of one cylinder when an additional cylinder is activated. Figure 19 shows the position of Cylinder A given a step input with the initial proportional control both before and after cylinder C is activated; the reduction in slope demonstrates the cylinder is no longer moving at the same velocity as previously and a correction in the control scheme is desired.

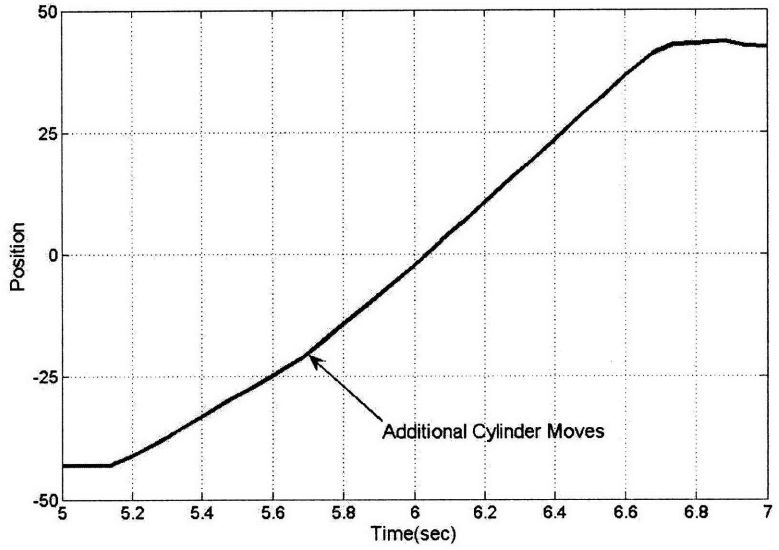

Figure 19: Another extension of this project would be to explore the behavior of one cylinder when an additional cylinder is activated. This figure shows the position of Cylinder A given a step input with the initial proportional control both before and after cylinder C is activated; the reduction in slope demonstrates the cylinder is no longer moving at the same velocity as previously and a correction in the control scheme is desired.

A theoretical explanation for this effect comes from considering basic fluid dynamics equations. The relationship between total fluid flow and cylinder flow is trivial when only one cylinder is in operation, but it naturally becomes more complex with multiple entities.[13] At any junction in a fluidic system, diagrammed in Figure 20, the total flow into the junction, Q_{total}, must equal that of the flow out, as in Equation 10. Further, the pressure in all three lines must be equalized, seen in Equation 11. These two constraints dictate that the pressure drop across valve A in Figure 20 must be controlled in tandem with valve B for

[13]White p. 343.

both to achieve the desired velocities with respect to one another.

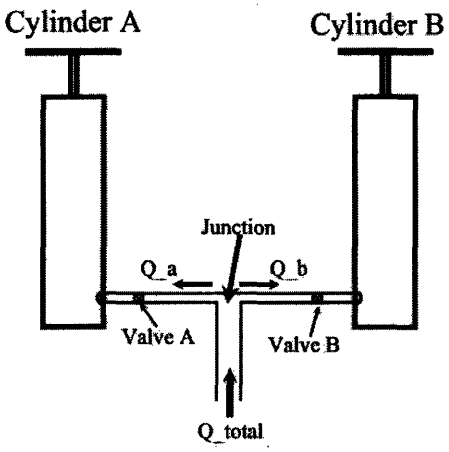

Figure 20: The relationship between total fluid flow and cylinder flow is trivial when only one cylinder is in operation, but it naturally becomes more complex with multiple entities. At any junction in a fluidic system, the total flow into the junction, Q_{total}, must equal that of the flow out, as in Equation 10. Further, the pressure in all three lines must be equalized, seen in Equation 11. These two constraints dictate that the pressure drop across valve A must be controlled in tandem with valve B for both to achieve the desired velocities with respect to one another.

$$Q_{total} = Q_a + Q_b \tag{10}$$

$$P_{system} = P_a = P_b \tag{11}$$

One final project consideration would be to expand the feed-forward command tables to include multiple pump pressures. All experiments in this thesis were carried out with the pump pressure controlled to a nominal 500psi (3.45MPa). In reality, there will likely be times wherein a higher system pressure is desired, perhaps to support an unusually heavy payload. It would be wasteful to continually maintain the higher pressure under normal operating conditions, and further experimentation would provide this added dimension to the command tables. All told, this thesis project has laid the groundwork for what will eventually be an extensive course of experimentation.

8 Conclusion

This thesis project characterized a Hydraforce SP08-47CL valve controlled by a pwm duty cycle. After building a test apparatus to reduce the effect of geometrical coupling, multiple tests were conducted to develop an empirical relationship between piston velocity and pwm command signal. A model of the system was then constructed to theoretically justify the experimental results. Having proved the soundness of the empirical model, low-order polynomials were fit to the data to produce an ultimately more practical solution.

As the development of the BEAR^{TM} robot continues, the feed-forward terms discussed in Figure 2(b) and similar equations as described by Table 1 will be implemented to improve upon BEAR^{TM}'s path-following capabilities. With these feed-forward terms, the cylinders will be less dependent upon the error term in the feed-back control scheme, resulting in increased response to directional change, less delay, and more efficient allocation of computational resources.

9 Bibliography

1. Akers, A., Gassman, M., & Smith, R. (2006). *Hydraulic power system analysis.* Boca Raton: Taylor & Francis Group, LLC.

2. Asada, H. H. *Actuators and drive systems.* Unpublished manuscript.

3. *Electro-proportional valves–directional control.* Retrieved February 12, 2008, from http://www.hydraforce.com/Proport/Prop-pdf/2-110-1.pdf

4. Nise, N. S. (2008). *Control systems engineering* (5th ed.). Hoboken, NJ: Wiley.

5. *Product & services: The BEAR^{TM} robot.* (2007). Retrieved March 29, 2008, from http://vecnarobotics.com/robotics/product-services/bear-robot/bear_details.shtml

6. Walters, R. B. (1991). *Hydraulic and electro-hydraulic control systems.* Essex: Elsevier Science Publishers LTD.

7. Watton, J. (2007). *Modelling, monitoring and diagnostic techniques for fluid power systems.* London: Springer-Verlag London Limited.

8. White, F. M. (2003). *Fluid mechanics* (5th ed.). New York: McGraw-Hill.